Department of Electrical
and
Computer Systems Engineering

Technical Report
MECSE-33-2004

A Venier Double Ring Shape-8 Optically Amplified Resonator

LN Binh

MONASH
UNIVERSITY

A VERNIER DOUBLE RING SHAPE-8 OPTICALLY AMPLIFIED RESONATOR

Le Nguyen Binh

Laboratory of Optical Communications and Applied Photonics, Department of Elctrical and Computer Systems Engineering, Monash University, Clayton, VICTORIA 3168 MELBOURNE AUSTRALIA

Abstract

We present the Vernier optical fiber Shape-8 double-ring resonator consisting of two optical fibre rings with a gain coupling cofficent path connecting the two rings. One of the ring is twisted to form an enclosed Shape-8. Photonic graphical techniques are applied to obtain the transfer functions between input and output ports of the photonic circuit. The Shape-8 Vernier Double Ring optical resonator (S8-VDR) is synthesised by using the z-domain optical transfer function. A very large effective free spectral range (FSR) and finesse can be obtained. The Vernier operation of the circuit is demonstrated with high peak resonance and wide spectral range.

TABLE OF CONTENTS

1. Introduction

Multiple optical resonators are well known of its infinite applications in high-performance optical fibre communication systems and ophotonic signal processing. An intracavity coupling laser[1] have attracted attention lately due its excellent in lasing charcterictics and sharp linewidth. An fibre optic or integrated optic forms of such configuration would offer a compact and high performance optical component. Such optical circuit can be constructed by using two optical couplers with their optical input and ouput ports interconnected as shown in Figure 1 to form an S-shaped double ring resonator. In addition the optical directional couplers can exhibit optical gains, such gain can be implemented using an EDFA. Furthermore a composite of these resonators operating under unstable conditions can be used to form another important class of resonators to generate high power composite lasers. These composite lasers can be formed by fibre laser cavities in bundle with partial coupling from one individual resonator to another with appropriate phase locking. The optical resonator illustrates such a double cavity coupled resonator. Intutively there are two main optical ring resonators formed by the outer and inner twisted rings. They are coupled to each other by the cross coupling of optical powers through the two couplers 1 and 2. the coupler 3 is used to tap the output power and to couple the optical power from other parrale resonators of the composite bundled laser.

The analysis of these coupled resonators is necessary for the implementation these multiple cavity coupled resonators. Such analysis if using the normal coupled field equations is complicated and requires large computing power [1]. In order to analyse such an optical circuit, it would be tedious to use derive a set of field equations which express the relationship between optical fields in the optical system. We thus propose a systematic method for computerisation. This paper thus aims to employ a graphical approach in the analytical derivation of the optical transfer functions of the Shape-8 Vernier Double Ring (S8-VDR) resonator. The graphical representation presented here for photonic circuits can be adapted from the well known signal flow graph (SFG) method for electrical circuits. The unique feature of our work is that optical circuits can be represented in SFG diagrams in a planar form in which there are no crossing between the signal flow paths, thus allowing us to apply Mason's rule to produce the equivalent photonic circuits [4].

A Vernier configuration has a periodic resonant characteristics in the frequency domain with the free spectral range (FSR) between the filter peaks given by

$$\mathrm{FSR} = \frac{\mathrm{N}}{\mathrm{N}+1} \tag{1}$$

with $\mathrm{N} \geq 2$, the resulting effective FSR will be increased significantly, while the full-width-half-maximum FWHM is greatly reduced [3] as similar to the case of a double-cavity Fabry-Perot (FP) filter. The Vernier resonators employing degenerate two-wave mixing and a single-coupler fibre ring resonator [5] and a double-coupler fibre ring-loop resonator [6] have been reported. The output of these resonators can change from being a channel-blocking type to a channel-passing type and the input signals are amplified as well. This can be achieved by connecting two couplers in two rings but with one of the rings is twisted (forming a '8' shape). The pumped signal would then be circulating within the two rings forming two forward waves and two backward waves and hence the degenerate four-wave mixing (DFWM). The connection of the optical circuit is shown in ***Figure 1***. The Vernier operation, which increases the effective FSR, will greatly enhance the applicability of the fiber rings as demultiplexers or filters in densely spaced WDM systems [7].

The graphical technique for analysing photonic circuits is presented in Section 2, followed by its application to obtaining the transfer function in Section 3. A detailed performance study of a S8-VDR will be carried out and its important features will be identified as an illustration of the efficiency of the developed graphical technique in Section 4. The design and implementation of S8-VDR will be concluded in Section 5.

2. Graphical Representation of Photonic Circuits

Optical couplers in photonic circuit can be represented and analysed graphically. However, only optical lumped circuits are analysed here and it is assumed that the circuits are linear and time-invariant. Furthermore, we assume a temporally incoherent system where light intensities are used instead of electric fields and we also assume that the coherence length of the laser source is very much shorter than the length of the delay paths so as to achieve resonance.

The input-output intensities relationship of a *2x2* optical directional coupler, whose schematic diagram is shown in ***Figure 2***(a), is governed by

$$\begin{bmatrix} I_3 \\ I_4 \end{bmatrix} = (1-\gamma)\begin{bmatrix} 1-k & k \\ k & 1-k \end{bmatrix}\begin{bmatrix} I_1 \\ I_2 \end{bmatrix} \quad (2)$$

where (I_1,I_2) and (I_3,I_4) are the input and output intensities at ports *1* and *2* and ports *3* and *4*, respectively, γ is the intensity coupling loss factor and *k* is the intensity coupling coefficient. We assume that the couplers are lossless ($\gamma = 0$) and symmetrical.

According to ***Figure 2***(a), the *2x2* optical directional coupler can be represented in a planar signal flow graph diagram shown in ***Figure 2***(b) where the light intensity from port *1* is transmitted to port *3* with a coupling factor of *(1-k)* and to port *4* with a cross-intensity coupling coefficient of *k*. Likewise for the case from port *2*. If complex electric fields are used, then a 90 degree phase shift between port *1* and port *4* or between port *2* and port *3* must be included in ***Figure 2***(b).

The schematic diagram of the S8-VDR optical resonator is shown in ***Figure 1***. Using the graphical representation for the couplers and by following the flow of the optical input signal I_1 at input port *1*, its signal flow graph representation can be obtained as shown in ***Figure 3***. Intensity coupling coefficients k_1, k_2 and k_3 denote the respective couplers in the circuit. The *z*-transform parameter is defined as :

$$z^{-1} = e^{j\beta L} = e^{j\omega T} \quad (3)$$

where β is the propagation constant of the guided fundamental mode in optical fibre loop and *T* is the unit-delay time of the fibre loop of unit length *L*. The delay of the three different delay paths are then expressed as the exponential coefficients d_1, d_2 and d_3. We can normalise the time to unit time *T* and hence the unit length *L*. Thus, $d_i=1$ corresponds to unit length *L*, $d_i=2$ corresponds to length *2L* and so on.

Since we consider the photonic circuit as a linear, discrete-time and time-invariant optical system, the delay length can be represented as z^{-d}. The unit delay is therefore represented as z^{-1}, delay of two unit is represented as z^{-2} and so on. The transmission coefficient of an optical path can be therfore defined as

$$t = G\exp(-2\alpha L) \quad (4)$$

where α is the attenuation coefficient of the fibre and G is the linear optical gain. A special erbium-doped fibre can be inserted in the delay paths to obtain the required optical amplifier gain factor G. The nodes denoted with primed numbers are used to denote lightwaves propagating in a direction opposite to those denoted by unprimed nodes.

3. Photonic Transfer Functions

Transfer function of S8-VDR optical resonator can be obtained graphically as demonstrated in this section. Systematic procedures of the determination of the transfer function can be illustrated in details in a number of articles [2]. However it is essential to briefly describe it here due to complexity of this coupled system of resonators.

3.1 Mason's Rule for optical circuits

Mason's rule states that the transfer function or input-output transmittance relationship between two nodes in a signal flow graph is given by

$$H = \frac{1}{\Delta}\sum_{i=1}^{n} T_i \Delta_i \tag{5}$$

where H = the network function relating an input and output port; T_i = the gain (transmittance) of the i-th forward (open) path from input to output; n = the total number of forward paths from input to output.

The symbol Δ denotes the signal flow graph determinant which is given as:

$$\Delta = 1 - \sum_{i} T_i + \sum_{i,j} T_i T_j - \sum_{i,j,k} T_i T_j T_k + \ldots \tag{6}$$

where the T_i is the i^{th} the loop transmittance gain and in each of the product summations in (6) only products of non-touching loops are included. The term non-touching implies loops which have no node in common, ie. separated loops. Note that the sign is minus for a sum of products of an odd number of loop gains and plus otherwise. The symbol Δ_i is the determinant Δ after all loops which touch the T_i path at any node have been eliminated. It is noted here that optical transmittance is used throughout our graphical representation.

3.2 Transfer Function of S8-VDR Optical Resonator

As mentioned before that k_1, k_2 and k_3 denote the coupling coefficients of the optical couplers. We acn also define that

$$a_i = t_i z^{-d_i} \tag{6}$$

The optical transfer function of the S8-VDR can now be found in the following steps:

***Step 1* :**

Search for all independent optical loop gain in ***Figure 3***. As a result of the complexity of S8-VDR structure, there are eighteen individual loop gains being obtained and all the loop gains are denoted as $L_1, L_2, L_3, ... , L_{18}$.

Refer to ***Figure 4***, we obtain the loop optical transmittance gain for loop *L(1-4)* as

$$L_1 = a_3^2(1-k_1)(1-k_2) \tag{7}$$

$$L_2 = a_3^2(1-k_1)(1-k_2) \tag{8}$$

$$L_3 = a_1^2 a_2 a_3^2 k_1^2 k_2^2(1-k_3) \tag{9}$$

$$L_4 = a_1^2 a_2(1-k_1)(1-k_2)(1-k_3) \tag{10}$$

Similarly refering to ***Figure 5*** for loops 5 and 6 we have

$$L_5 = a_1^2 a_2(1-k_1)(1-k_2)(1-k_3) \tag{11}$$

$$L_6 = a_1^2 a_2 a_3^2 k_1^2 k_2^2(1-k_3) \tag{12}$$

It follows that the loop gains for loops 7 to 18 can be obtained by refering to ***Figure 6*** to ***Figure 11*** we can obtain the path transmission coefficient as:

$$L_7 = a_1^2 a_2 a_3^4 k_1^2 k_2^2(1-k_1)(1-k_2)(1-k_3) \tag{13}$$

$$L_8 = a_1^2 a_2 a_3^2 k_2^2(1-k_1)^2(1-k_3) \tag{14}$$

$$L_9 = a_1^2 a_2 a_3^2 k_1^2 (1-k_2)^2 (1-k_3) \quad (15)$$

$$L_{10} = a_1^2 a_2 a_3^4 k_1^2 k_2^2 (1-k_1)(1-k_2)(1-k_3) \quad (16)$$

$$L_{11} = a_1^4 a_2^2 a_3^4 k_1^4 k_2^2 (1-k_2)^2 (1-k_3)^2 \quad (17)$$

$$L_{12} = a_1^4 a_2^2 a_3^2 k_1^2 k_2^2 (1-k_1)(1-k_2)(1-k_3)^2 \quad (18)$$

$$L_{13} = a_1^4 a_2^2 a_3^4 k_1^2 k_2^4 (1-k_1)^2 (1-k_3)^2 \quad (19)$$

$$L_{14} = a_1^4 a_2^2 a_3^2 k_1^2 k_2^2 (1-k_1)(1-k_2)(1-k_3)^2 \quad (20)$$

$$L_{15} = a_1^4 a_2^2 a_3^4 k_1^2 k_2^4 (1-k_1)^2 (1-k_3)^2 \quad (21)$$

$$L_{16} = a_1^4 a_2^2 a_3^4 k_1^4 k_2^2 (1-k_2)^2 (1-k_3)^2 \quad (22)$$

$$L_{17} = a_1^2 a_2 a_3^2 k_2^2 (1-k_1)^2 (1-k_3) \quad (23)$$

$$L_{18} = a_1^2 a_2 a_3^2 k_1^2 (1-k_2)^2 (1-k_3) \quad (24)$$

As the S8-VDR optical resonator is a symmetrical linear time-invariant system, we expect that there are nine pairs of independent loop gains which are tabulated in ***Table 1***. Thus, we can see the two pairs of degenerate two wave mixing (DTWM) which form the degenerate four wave mixing (DFWM). The optical gain obtained through this DFWM is approximately euqual for both directions of the propagation of the lightwaves. Similarly in-line fibre ampliofiers such the Er:doped silica fibre can be pumped in co- or contra-direction.

Nine Pairs of Loop Gain			
L_1 & L_2	L_3 & L_6	L_4 & L_5	L_7 & L_{10}
L_8 & L_{17}	L_9 & L_{18}	L_{11} & L_{16}	L_{12} & L_{14}
L_{13} & L_{15}			

Table 1 List of the paired loop gains of S8-VDR optical resonator

***Step 2* :**

Analyse the loops in ***Figure 3*** graphically and find the signal flow graph's determinant Δ which has been defined in (6). Thus, we obtain

$$\sum_{i} T_i = L_1 + L_2 + L_3 + L_4 + L_5 + L_6 + L_7 + L_8 + L_9 + \ldots \\ L_{10} + L_{11} + L_{12} + L_{13} + L_{14} + L_{15} + L_{16} + L_{17} + L_{18} \quad (25)$$

$$\sum_{i,j} T_i T_j = L_1L_2 + L_1L_4 + L_1L_5 + L_1L_9 + L_1L_{12} + L_1L_{17} + \ldots \\ L_2L_4 + L_2L_5 + L_2L_8 + L_2L_{14} + L_2L_{18} + \ldots \\ L_3L_6 + L_4L_5 + L_4L_7 + L_4L_8 + L_4L_9 + \ldots \\ L_5L_{10} + L_5L_{17} + L_5L_{18} + L_8L_{17} + L_9L_{18} \quad (26)$$

$$\sum_{i,j,k} T_i T_j T_k = L_1L_2L_4 + L_1L_2L_5 + L_1L_4L_5 + L_1L_4L_9 + \ldots \\ L_1L_5L_{17} + L_2L_4L_5 + L_2L_4L_8 + L_2L_5L_{18} \quad (27)$$

$$\sum_{i,j,k,l} T_i T_j T_k T_l = L_1L_2L_4L_5 \quad (28)$$

and hence, Δ can be found easily by substituting (26), (27), (28) and (29) into (6).

***Step 3* :**

Finally, we have to find the forward paths from node *1* to node *3* denoted by T_i and its determinant Δ_i which corresponds to non-touching loops.

$$T_1 = (1 - k_3) \quad (29)$$

$$\Delta_1 = 1 - (L_1 + L_2 + L_3 + L_4 + L_5 + L_6 + L_7 + L_8 + L_9 + \ldots \\ L_{10} + L_{11} + L_{12} + L_{13} + L_{14} + L_{15} + L_{16} + L_{17} + L_{18}) \quad (30)$$

$$T_2 = a_1^2 a_2 k_3^2 (1 - k_1)(1 - k_2) \quad (31)$$

$$\Delta_2 = 1 - (L_1 + L_2 + L_4 + L_{10} + L_{17} + L_{18}) \quad (32)$$

$$T_3 = a_1^2 a_2 a_3^2 k_1^2 k_2^2 k_3^2 \quad (33)$$

$$\Delta_3 = 1 - L_3 \tag{34}$$

$$T_4 = a_1^2 a_2 a_3^4 k_1^2 k_2^2 k_3^2 (1-k_1)(1-k_2) \tag{35}$$

$$\Delta_4 = 1 - L_4 \tag{36}$$

$$T_5 = a_1^2 a_2 a_3^2 k_2^2 k_3^2 (1-k_1)^2 \tag{37}$$

$$\Delta_5 = 1 - (L_2 + L_4 + L_{17}) \tag{38}$$

$$T_6 = a_1^2 a_2 a_3^2 k_1^2 k_3^2 (1-k_2)^2 \tag{39}$$

$$\Delta_6 = 1 - (L_1 + L_4 + L_{18}) \tag{40}$$

$$T_7 = a_1^4 a_2^2 a_3^4 k_1^4 k_2^2 k_3^2 (1-k_2)^2 (1-k_3) \tag{41}$$

$$\Delta_7 = 1 \tag{42}$$

$$T_8 = a_1^4 a_2^2 a_3^2 k_1^2 k_2^2 k_3^2 (1-k_1)(1-k_2)(1-k_3) \tag{43}$$

$$\Delta_8 = 1 - L_1 \tag{44}$$

$$T_9 = a_1^4 a_2^2 a_3^4 k_1^2 k_2^4 k_3^2 (1-k_1)^2 (1-k_3) \tag{45}$$

$$\Delta_9 = 1 \tag{46}$$

$$T_{10} = a_1^4 a_2^2 a_3^2 k_1^2 k_2^2 k_3^2 (1-k_1)(1-k_2)(1-k_3) \tag{47}$$

$$\Delta_{10} = 1 - L_2 \tag{48}$$

$$T_{11} = a_1^4 a_2^2 a_3^4 k_1^2 k_2^4 k_3^2 (1-k_1)^2 (1-k_3) \tag{49}$$

$$\Delta_{11} = 1 \tag{50}$$

$$T_{12} = a_1^4 a_2^2 a_3^4 k_1^4 k_2^2 k_3^2 (1-k_2)^2 (1-k_3) \tag{51}$$

$$\Delta_{12} = 1 \tag{52}$$

Hence, by substituting (26)-(52) into (5), we can obtain the transfer functions between the inpout and output ports of the S8-VDR resonator. The above analysis can easily be adapted to the case for coherent resonance system of the S8-VDR where the optical fields are used instead of the intensity representation of the couplers. In this case the coupling matrix of (1) is replaced with the input and output fields $E_{1....}$ E_4 for the intensities I_1 ... I_4 respectively. The coupling coefficients are replaced by $-jk_i$ for the cross coupling or the off-diagonal component and $(1-k_i)^{1/2}$ for the diagonal components where k_i indicates the optical power coupling coeffcients ofthe three couplers. It is thus very straight forward to obtain the optical transfer functions for the S8-VDR operating under coherent conditions. This paper reports the results of the analysis for a temporally incoherent resonators that satisfy the condition for composite or multiple and bundle optical resonance system. These are described in the next section.

4. Results and Discussions

In this section, the analysis of the behaviour of S8-VDR optical resonator is presented. Application of S8-VDR has been suggested. The free spectral range (FSR) is discussed. The Vernier operation is demonstrated.

4.1 The Effect of the Delay Paths to the behaviour of S8-VDR

S8-VDR optical resonator is synthesised by setting all the coupling coefficients and optical amplifier gains equal to 0.2 and 1 respectively. Referring to ***Figure 3***, the three delay paths are denoted as d_1, d_2 and d_3. The delay for the inner twisted loop is assumed to be the same for both branches of the ring. By varying these delay paths, we can observe many interesting characteristics.

4.1.1 Case (a) : Symmetry Topology with Equal Length

As we can observe in *Figure 12* that the S8-VDR optical resonator is resonating at different frequencies depending on the length of the delay path. In anoter word the order of the denominator and numerator of the optical transfer function is dependent on the delay orders of the optical paths. Thus it gives different singular points and zero points of the transmittance or the destructiveand constructive inteference at the output optical port. We term the singular points as the poles of the optical system and zeros as the depletion.

The search of the poles for maximum resonace is quite easy based on the condition that when the poles are on the unit circle in the z-plane, resonance will occur. This can be done numerically by plotting the locus of the poles by keeping all parameters constant but one. The intersection between this locus and the unit circle determines the resonance condition. For example of the conditions for operating the S8-VDR are kept the same as in *Figure 12* except that the gain g1 in the path d1 is now increased to 1.2 then the two poles in the far right of the pole-zero pattern in the z-plane are placed very closed to the unit circle. This gives a significant increase ofthe peak resonace and reduction in the parasitic peaks. The amplitude of the intensity gain is illustrated in ***Figure 13***(a) and its corresponding pole-zero pattern shown in ***Figure 13***(b). The resonance peak can easily be found by adjusting the gain g_3 to 1.038 through the locus search. Intutively this resonance of the S8-VDR is significantly improved when the parameters of the twisted inner loop is adjusted such that the total energy is conserved and a phase matching between all the forward paths from the input port 1 to ouput port 3. That is to compensate for the coupling of the energy through the two couplers 1 and 2 as well as a maximum interference of all the lightwaves paths. This is done by setting the gain g_3 to 1.038. The amplitude response and its corresponding pole-zero plots are shown in ***Figure 14***(a) and (b). Throughout this paper the scale of the intensity scale is assigned without unit as it is the intensity ratio gainn between the output port and the intensity at the input port which is set to 1.0 mW. The resonnance peak approaches nearly 1,500. the paek is very close to zero due to a pair of pole at the origin which are very close to each other. The separation between these poles determines the bandwidth of the resonant filter.

The resonance of the S8-VDR can be enhanced by increasing the order of delay between the optical loops, the outer and twisted inner ones so that there is a total balance of the energy between these loops. This can be implemented by doubling the delays d1 and d2 of the outer loop. The relative intensity response and its corresponding pole-zero pattern are shown in ***Figure 15***. The pole-zero pattern is completely balanced with two pole pairs in the far right and left are symmetrical and close to the unit circle in the z-plane. The second resonant peak appears in the intensity response curve and the peak reaches an extremum of more than 2,500. Thus the FSR of the resonator is significantly increased. We note here that the delay can be varied accordingly between the two resonant loops in an integer number of unit delays. The oprder of delays d_1, d_2 *and* d_3 must take integer values so that the z-

transformation is hold. In practice and in case that the optical field equations are derived the βL and ωT are different between the two loops. This can be easily implemented by varying the delay orders of the two loops. Thus in our analysis the FSR is in fact normalised to 2π circle. Other parasiticpeaks can appear inside this range and the true FSR is scaled by multiplying the normalised FSR to the ration between the order of the delays of the two resonant loops.

When the parameters of the S8-VDR are kept the same as those of ***Figure 15*** except that the gain g_2 of the outer resonant loop is increased to 2, the three poles near the unit circle of the pole-zero pattern moves to become all real with twelve pole now inside the unit circle and the other four are well inside. This leads to lowering the resonant peak and the system becomes unstable because the poles have now been outside the unit circle. Unstable resonators however are classifed as important resonators for applications as composite lasers. Parasitic peaks have also been observed.

4.1.2 Case (b) : Symmetry Topology with Larger Delay Length in d_3

As the length of third delay path d_3 of the inner twisted loop is double, the number of resonating frequency increases. In this case there are additional poles appearing at the north and south poles of the unit circle. There is no symmetry ofthe pole-zero pattern with respect to the centre of the unit circle inthe z-plane. Thus we can observe a few more sub-FSRs if the third delay path is increased. These peaks are much smaller than the resonant peaks generated by the outer loop under resonance. These are shown in ***Figure 17***.

The main FSR is independent of d3. For d_3=5, one additional FSR appears as FSR1. On the other hand, there are many other newly evolved sub-FSRs. However the peakks of each resonant is decreased as d3 is increased. Thus as we decreased d3 there is a possibility to use the S8-VDR as a multimode laser source. From the pole-zero plot in ***Figure 18***, longer delay path such as d_3 will create more poles nearby the unit circle and hence more resonanting frequencies. The FSR for the outer loop can thus be increased by a factor of 5.

4.1.3 Case (c) : Asymmetry Topology with Different Delay Path

By setting different path lengths, we would not observe any sub-FSRs as in C*ase(b)*. However, as the length of the delay paths increases, the main FSR decreases. In *case(c)*, by doubling the length in each of the delay paths causes the FSR to reduce to half. Also, the full width half maximum (FWHM) of the peak is getting smaller as the path length increases. Thus, we can tune the resonator by having longer delay path. It can be used as the tunable laser source. Shown in ***Figure 17*** is the corresponding poles-zeros, magnitude and phase plot.

4.2 The Effect of the Coupling Coefficients to the behaviour of S8-VDR

S8-VDR optical resonator is synthesised by setting all the delay paths and optical amplifier gains equal to 2 and 1 respectively. As we can observe in ***Figure 18***, the coupling coefficient does play an important part to the resonant peaks. Smaller coupling coefficient would tend to suppress the parasitic peaks and place all the energy in the resonant peaks. This is the efefect of coupling to the forward and reversed waves propagating between the two resonant loops. The equal delay length of an oder 2 makes the coupling equally feedback and forth between these two resonators rings. As we can see the resonant peaks of $k=0.1$ overshoot to *800* in magnitude. The magnitude of resonant peaks decreases with the increase of the coupling coefficient. Also, all the unwanted parasitic peaks are amplified for $k \geq 0.2$.

It is no doubt that larger coupling coefficient is desirable for a single optical coupler but for the case of S8-VDR optical resonator, we want low value of coupling coefficient in order to have sharp resonant peaks. Furthermore, the full width half maximum (FWHM) can be minimised by using coupler with small coupling coefficient. Thus, S8-VDR optical resonator with this configuration can be used as high-speed laser source with tiny laser line-width which corresponds to the FWHM.

The resonant peaks and thus the optical filter bandwidth can be tuned by adjusting the optical gains g1 to 1.1 to compensate for the optical energy coupled out of the loop and g_3 to 1.038 to force the poles of the system very close to the unit circle of the z-plane. Thus we observe that the optical bandwidth situated near the centre of the wT axis can be tuned with a very sharp cut off. This is the main feature of the S8-VDR in that a complete balance of the optical energy can be achieved by balancing the pole and zero pattern or the interference of the lightwaves circulating in the two resonant

loops with a coupling of energy in the twp loops to the forward of reverse waves propagating in them. We note also that all the poles are inside the unit circle with some are very close to unity value. Thus the S8-VDR is under marginally stable region.

The poles at the north and south poles can be tuned on the unit circle of the z-plane by increasing the order of the delay d_3 to much higher than that of d_1 and d_2. In the case taht d3=20 the resonace curve is observed in ***Figure 20***(a) and its corresponding pattern in ***Figure 20***(b). This is significant for practical purpose that if the length of the optical fibre path d3 can be much longer than that ofthe outre loop to operate the S8-VDR as a sharp filter or any minute change in the delay path would not affect its resonance behaviour. This due to the fact that the zeros are generated with the poles and pole-zero pairs. When the order of delay d_3 is very much larger than those of d_1 and d_2 the zeros are not at 0 or π are positioned very close to the pole and cancel its effect. This leads to two significant resonant peaks as observed in ***Figure 20***.

The effect of large difference between the delay length ofthe two resonant loops can also be observed with the order d_1 and d_2 of 20 while d_1 is set at 2. The relative intensity response as a function of the beta-length product is shown in Figure 22. A Vernier resonance is clearly shown. An FSR of about 155 is estimated which is far the largest for compund resonantors. The delay length ofth eouter ring as compared to that ofthe twisted inner ring has a great implication for implementing the S8-VDR in integrated optic form. Such an integrated optic device S8-VDR can be fabricated using the advanced-silica polymeric epitaxial chemical vapour deposition techniue. The high index rectangular optical waveguide can be buried in a lower silica index substrate.

The resonant frequency of each ring depends on the ring resonantor. Typical length for the shorter length ring resonator can be of order of 1.5 to 1.75 mm corresponding to an optical resoannt frequency of about 14.7 GHz. Thus a length difference of an order of 20 times would result to an approprimate free spectral range of about 281 GHz which is the largest for all ring resonators.

4.3 Effects of Optical Amplifier Gains

The effects of the optical gains ofthe two main paths for compensating the energy coupled S8-VDR optical resonator is synthesised by setting all the coupling

coefficients and delay paths equal to *0.2* and *2* respectively. In this experiment, the Vernier operation is achieved for the configuration where $g_1=g_3=1$ and $g_2=2$. In other words, the effective FSR is increased significantly. Compare ***Figure 20***(b) with *Figure 12*(b), the effective FSR or the magnitude of the resonant peaks is increased by ten times. Furthermore, the line-width is narrowed significantly by the DFWM (degenerate four wave mixing) and the resultant effective finesse (= FSR/FWHM) can be very large. Thus, when the gain is set closer to the Vernier gain, all the parasitic peaks diminish and energy will be channelled into the resonant peaks. As we can see in ***Figure 20***, *Vernier* operation starts to take effect at $g=1.5$. As we continue to increase the gain to *2*, it will reach to the *Vernier operation* point as shown in ***Figure 20***(b). However, further increase in gain will destroy the *Vernier operation.*

5. Conclusions

A theoretical analysis of S8-VDR optical resonator has been carried out and its important features have been identified. The important structural parameters that could affect the characteristic of S8-VDR have been analysed. The length of the delay paths can be adjusted to tune the resonator to the desire frequency. Coupling coefficient can be reduced in order to have sharper and larger resonant peaks which in turn producing a very narrow line-width. S8-VDR optical resonator can be further improved by driving the circuit into Vernier operation using the variable optical gain amplifier. Once the right gain is adjusted, all the energy from the parasitic peaks will be channelled into the resonant peaks. In our design under Vernier operation, the magnitude of the resonant peaks is increased significantly to ten times.

We have thus demonstrated by the simulation that the Vernier operation can be achieved with S8-VDR optical resonator by using degenerate four way mixing (DFWM). A very large effective FSR and finesse can be obtained. The implementation of the resonators are conducted and experimental results will be reported in the near future.

References

[1] Y. H. Ja, 'Vernier Fiber Double-Ring Resonator Using Degenerate Two-wave Mixing', *Micrrowave and Optical Technology Letters*, Vol.5, No.4, April 1992.

[2] L. N. Binh et. al., 'Graphical Representation and Analysis of the Z-Shaped Double-Coupler Optical Resonator', *IEEE Journal of Lightwave Technology*, November 1993.

[3] P. A. Humblet and W. M. Hamdy, 'Crosstalk Analysis and Filter Optimisation of Single-and-Double-Cavity Fabry-Perot Filters', *IEEE Journal of Selected Areas in Communications*, Vol.8, pp.1095-1107, 1990.

[4] S. J. Mason, 'Feedback theory - further properties of signal flow graphs', *Proceeding IRE*, Vol.44, pp.920-926, 1956.

[5] Y. H. Ja, 'Single-mode Optical Fibre Ring and Loop Resonators using Degenerate Two-Wave Mixing', Appl. Opt., Vol.30, pp.2424-2426, 1991.

[6] Y. H. Ja, 'A Double-Coupler Optical Fibre Ring-Loop Resonator with Degenerate Two-Wave Mixing', Opt. Commun., Vol.81, pp.113-122, 1991.

[7] B. S. Glance et. al., 'WDM Coherent Optical Star Network', J. Lightwave Technology, Vol.6, pp.67-72, 1988.

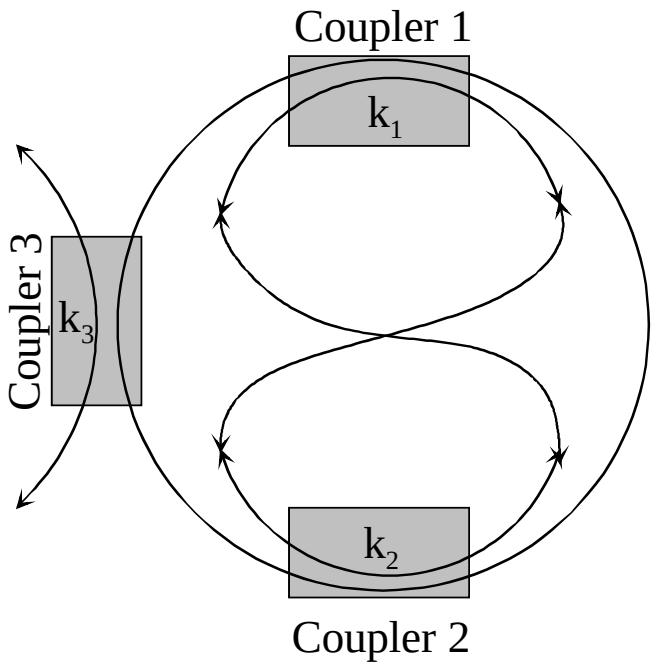

Figure 1 Shape-8 Vernier Double Ring (S8-VDR) optical resonator

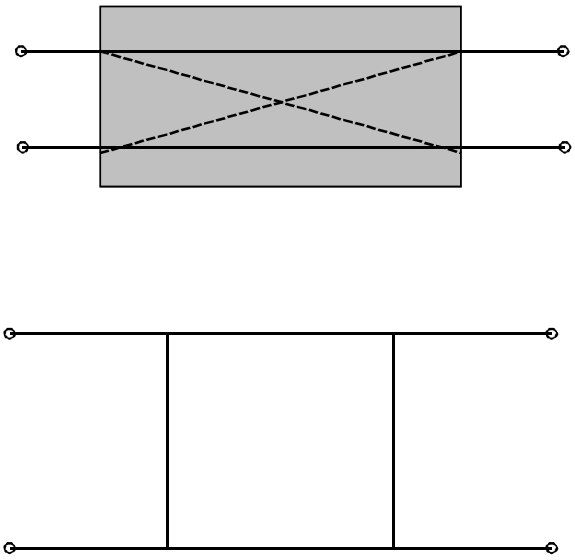

Figure 2 (a) Schematic diagram of a 2x2 optical directional coupler(b) Signal flow graph representation of a 2x2 optical directional coupler

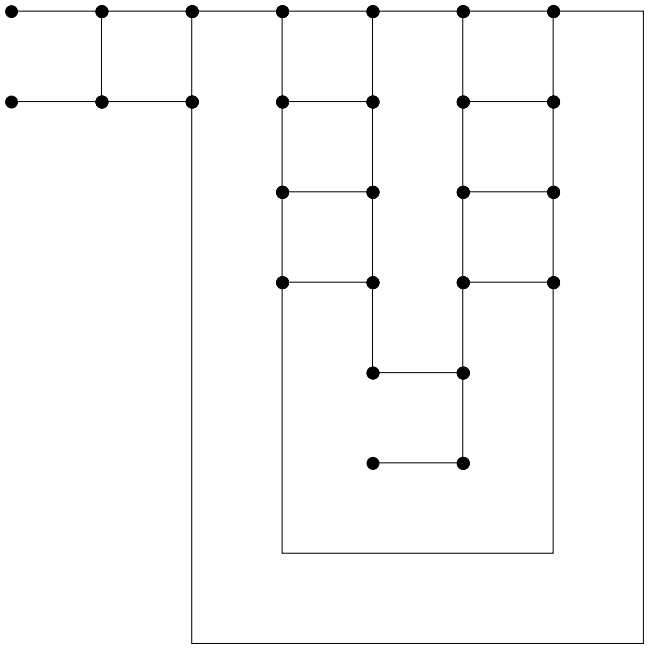

Figure 3 Schematic diagram of a S8-VDR optical resonator

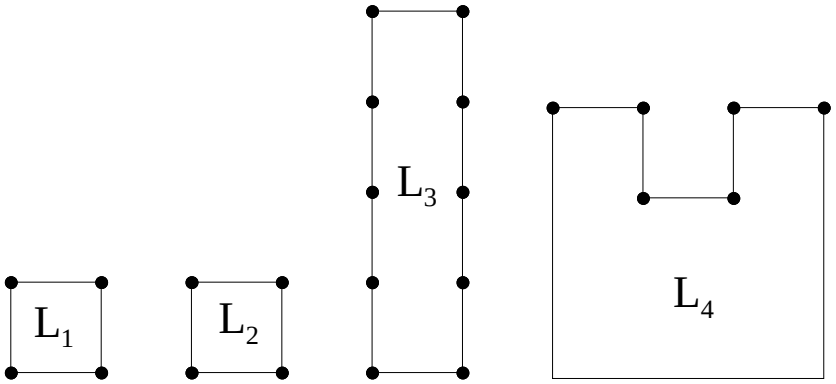

Figure 4 Independent optical loop gains for S8-VDR optical resonator

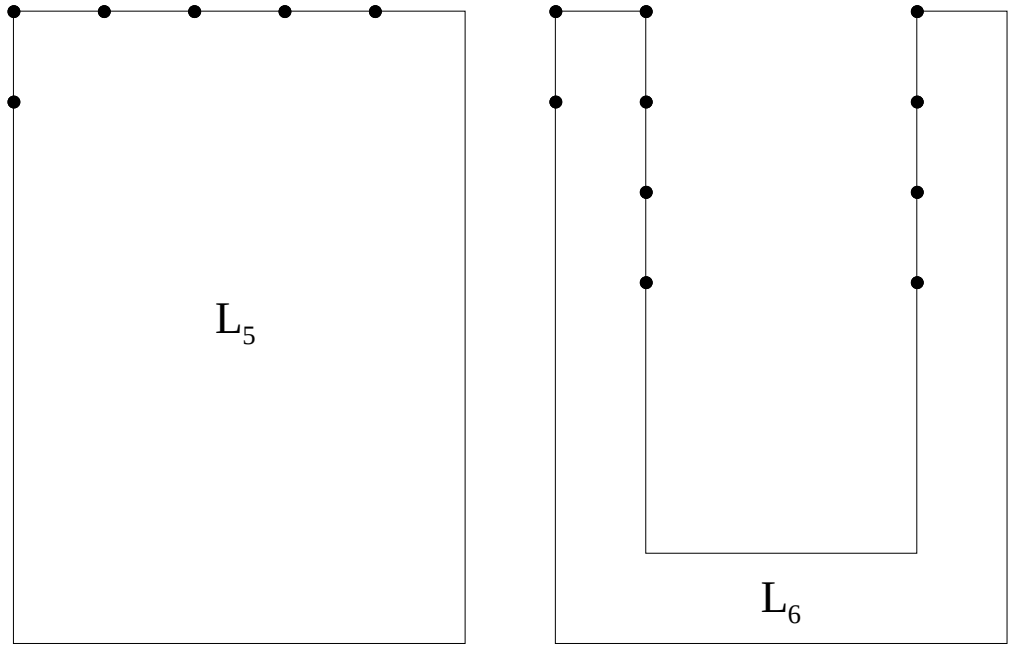

Figure 5 Independent optical loop gains for S8-VDR optical resonator

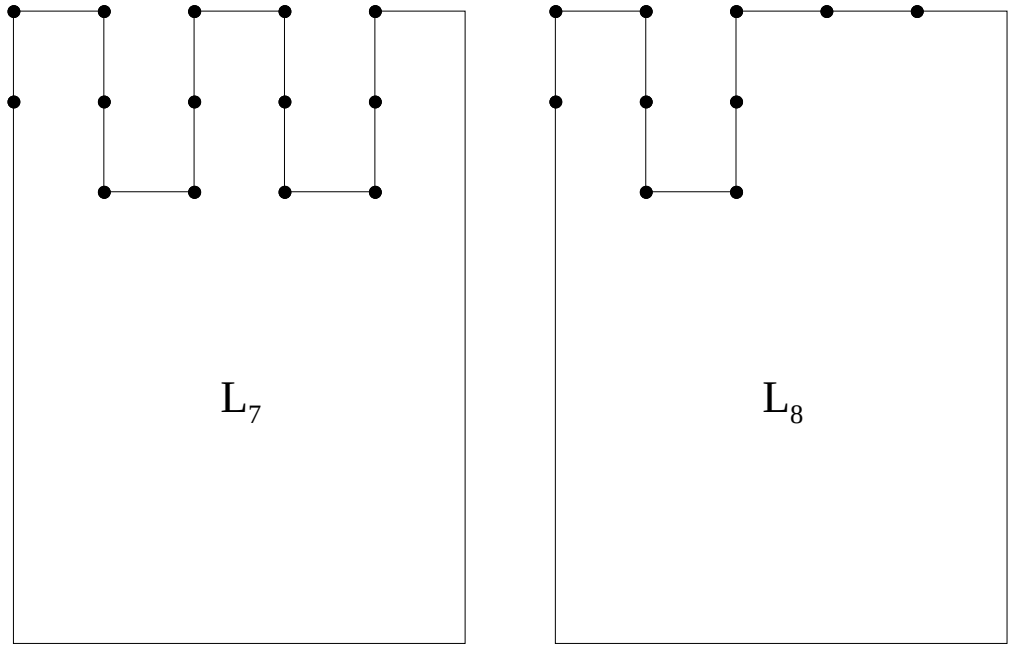

Figure 6 Independent optical loop gains for S8-VDR optical resonator

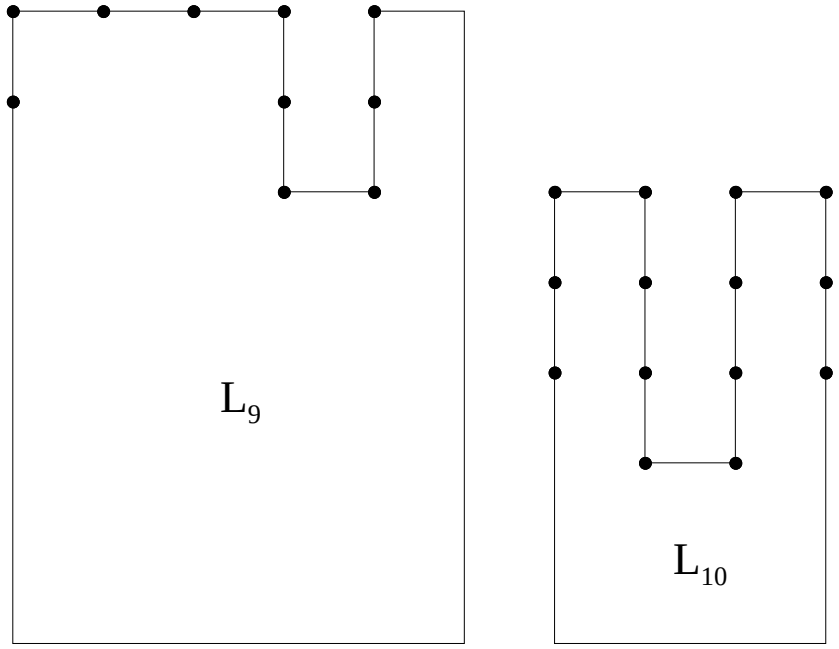

Figure 7 Independent optical loop gains for S8-VDR optical resonator

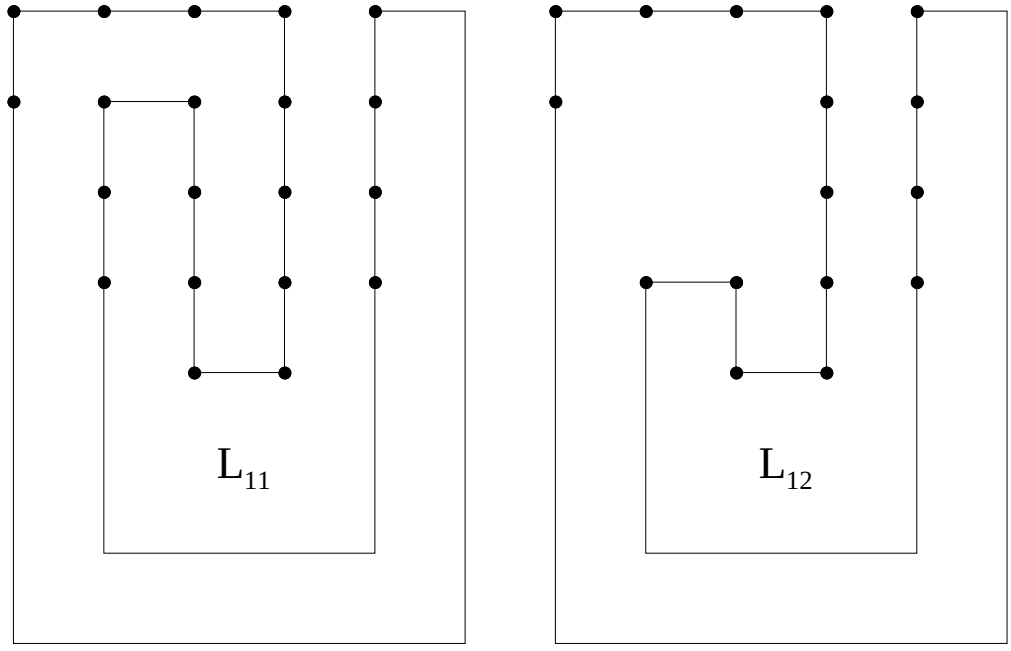

Figure 8 Independent optical loop gains for S8-VDR optical resonator

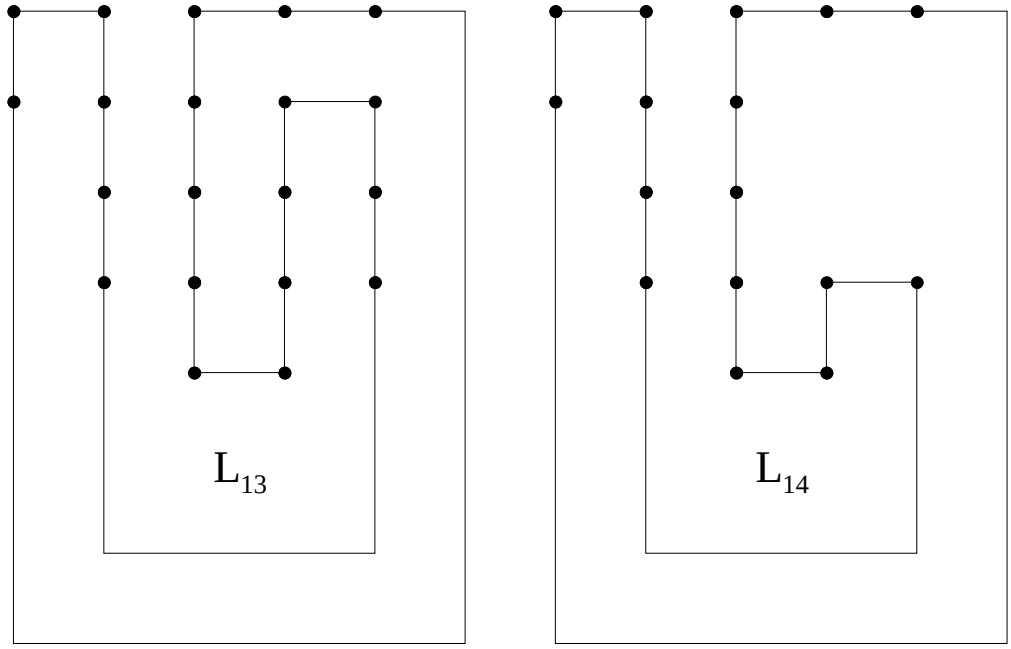

Figure 9 Independent optical loop gains for S8-VDR optical resonator

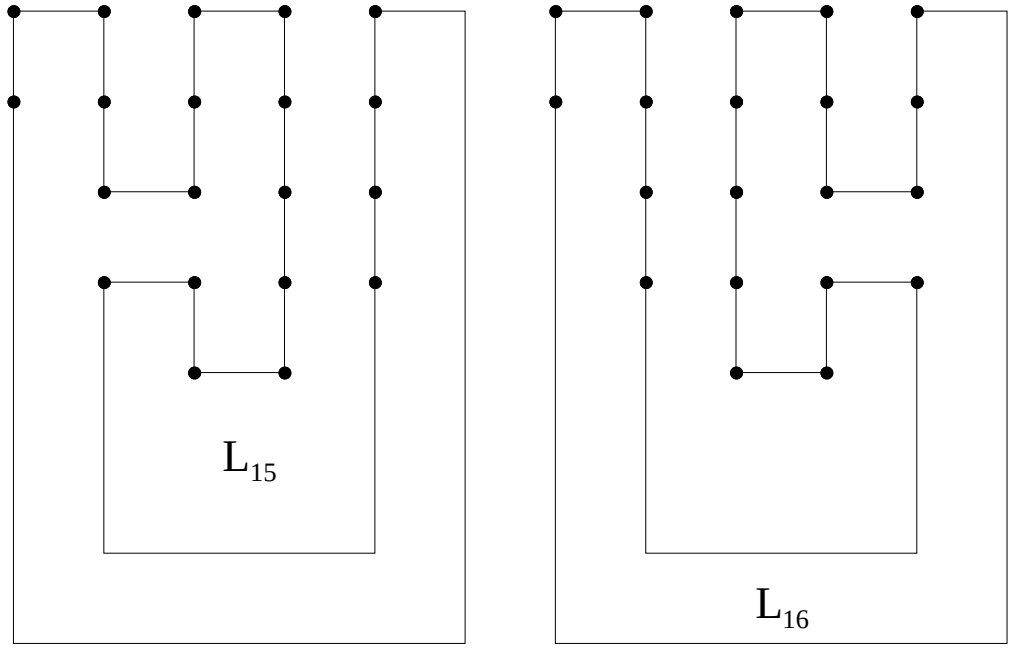

Figure 10 Independent optical loop gains for S8-VDR optical resonator

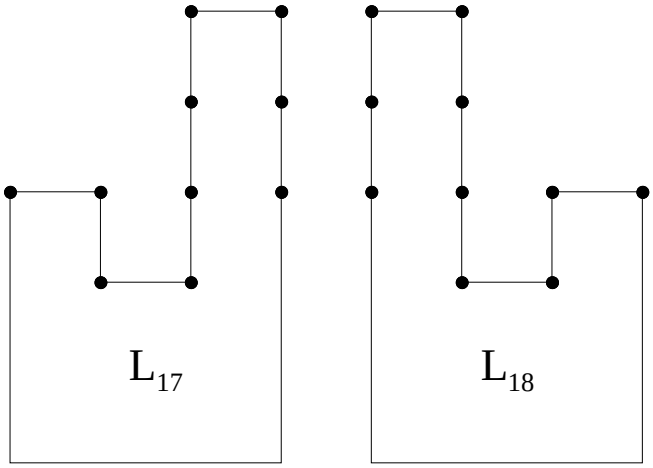

Figure 11 Independent optical loop gains for S8-VDR optical resonator

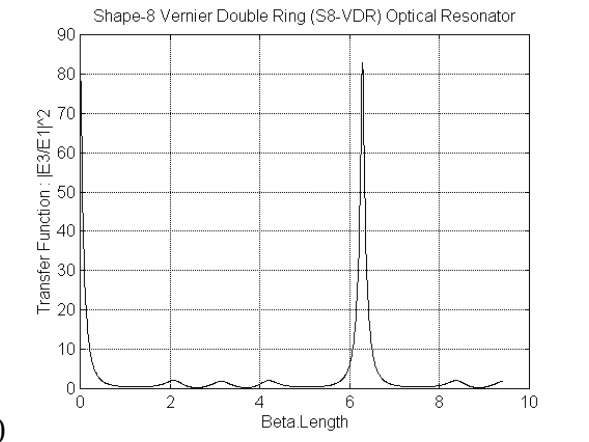

(a)

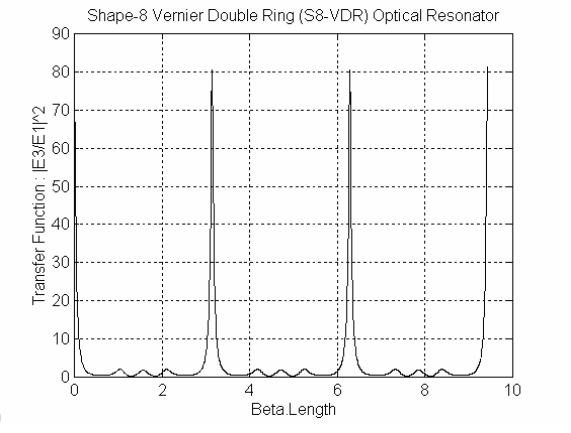

(b)

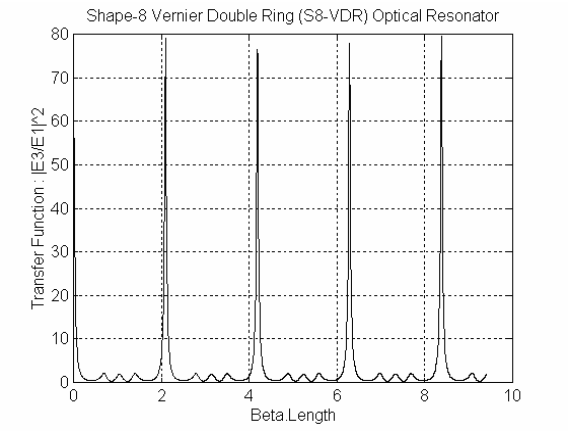

(c)

Figure 12 Optical filter transfer characteristics with (a) $d_1=d_2=d_3=1$ (b) $d_1=d_2=d_3=2$ and (c) $d_1=d_2=d_3=3$

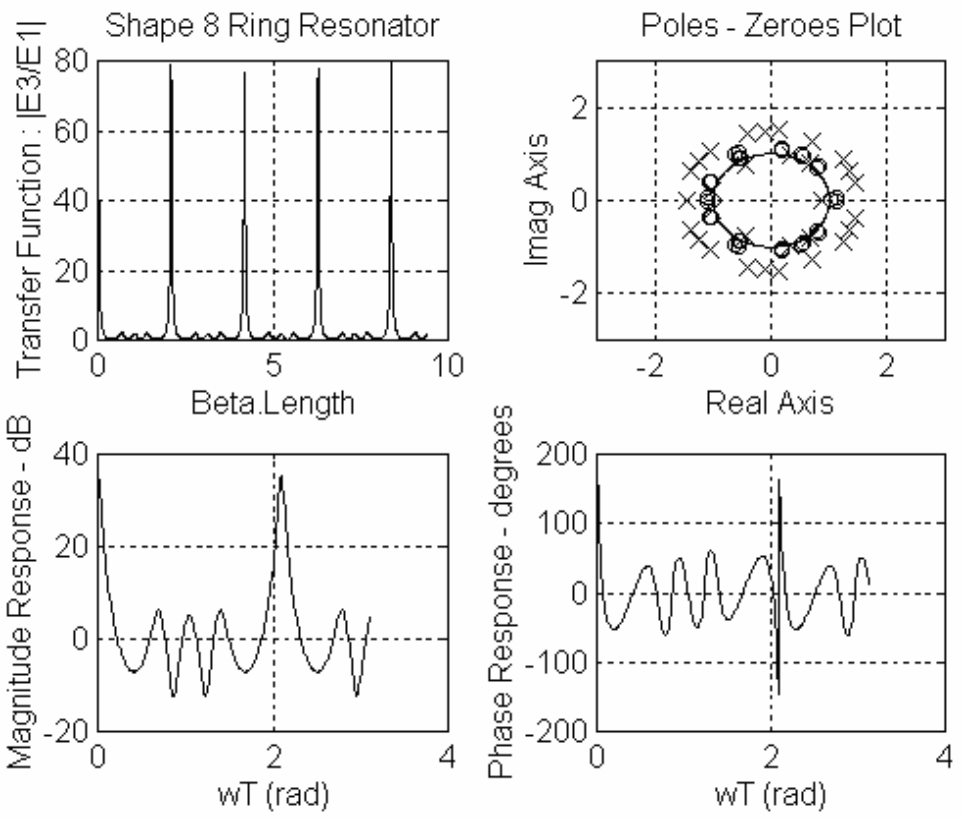

Figure 13 Optical transfer characteristics for the case of $d_1=d_2=d_3=3$

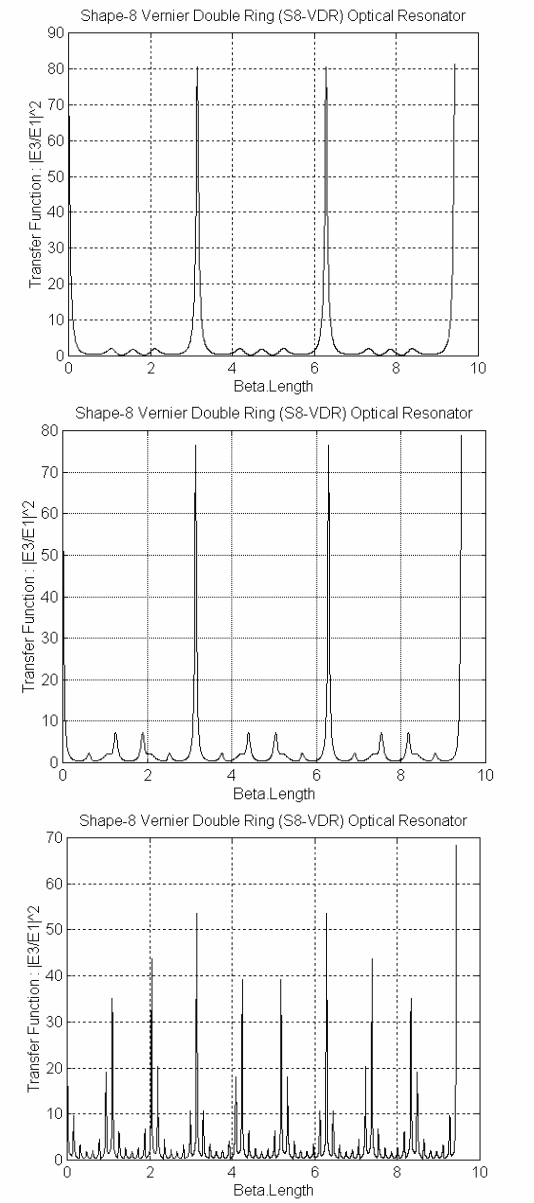

Figure 14 Optical transfer characteristics for the case of (a) $d_1=d_2=2$, $d_3=2$ (b) $d_1=d_2=2$, $d_3=5$ and (c) $d_1=d_2=2$, $d_3=20$

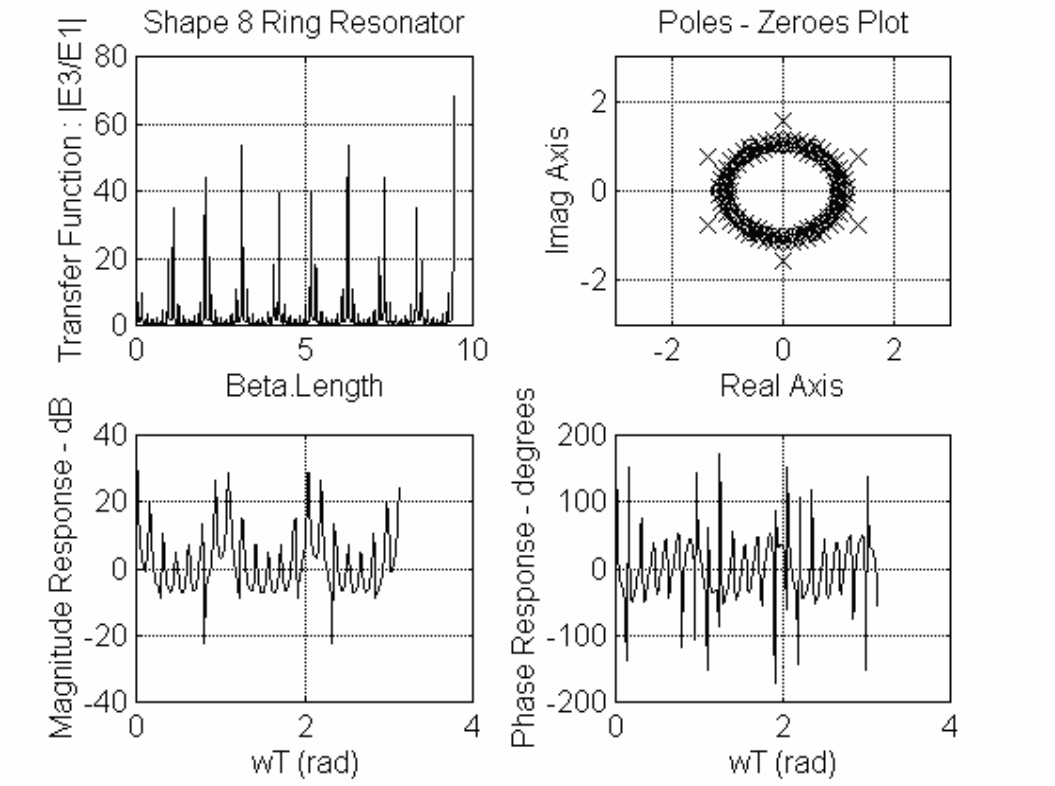

Figure 15 The optical transfer characteristics, pole-zero pattern and phase responss for the case of $d_1=d_2=2$, $d_3=20$

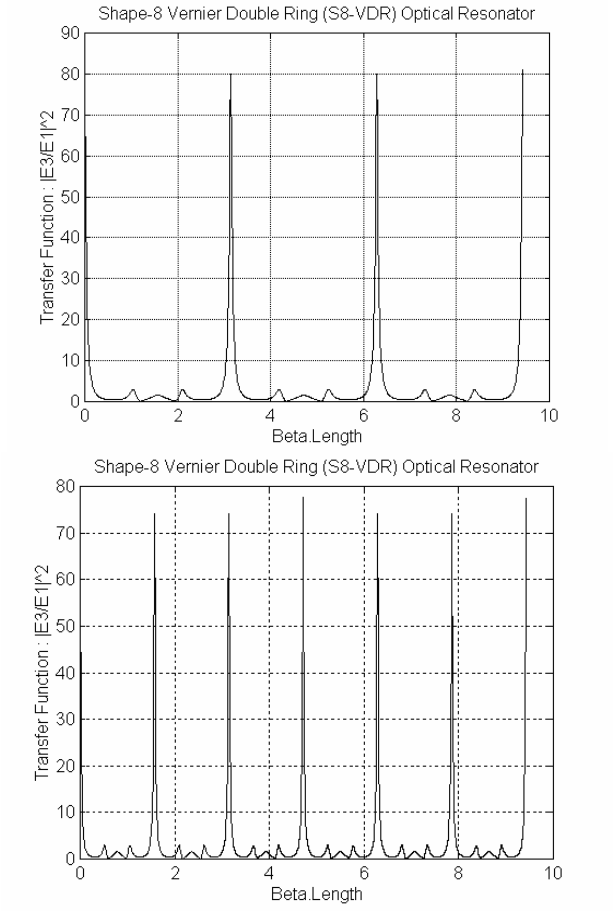

Figure 16 Optical Transfer Chracteristics for (a) d_1=1, d_2=2, d_3=3(b) d_1=2, d_2=4, d_3=6

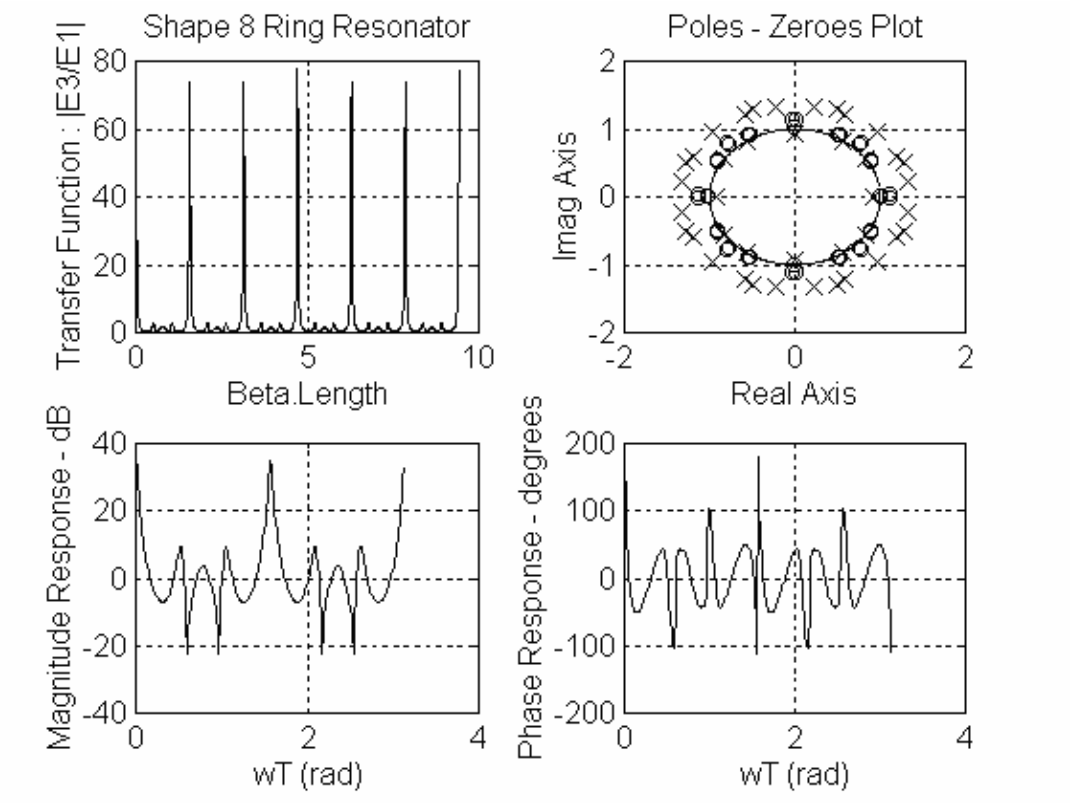

Figure 17 Optical transfer characteristics, pole zero patten and magnitude and phase responses for d_1=2, d_2=4, d_3=6

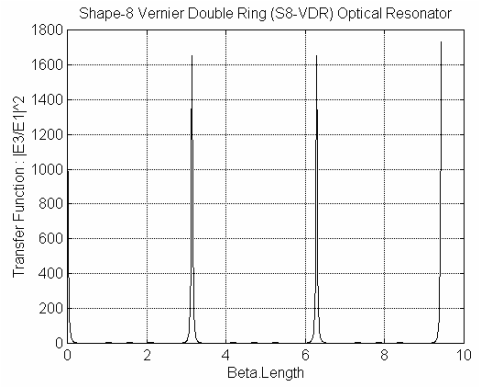

(a)

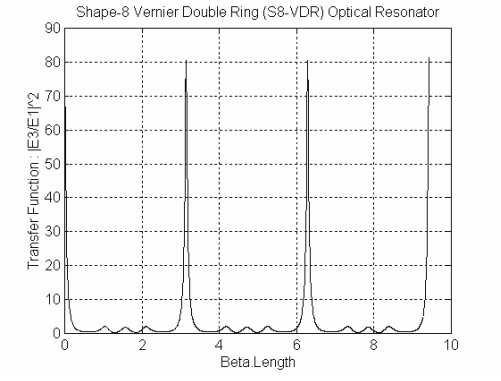

(b)

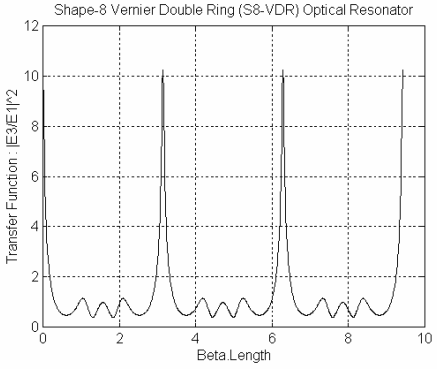

(c)

Figure 18 Optical transfer characteristics for (a) $k_1=k_2=k_3=0.2$ (b) $k_1=k_2=k_3=0.2$ and (c) $k_1=k_2=k_3=0.3$

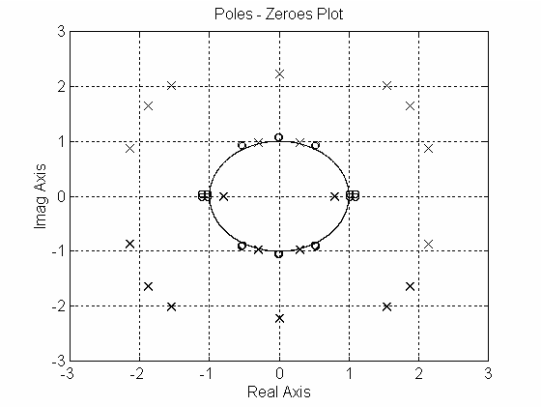

(a)

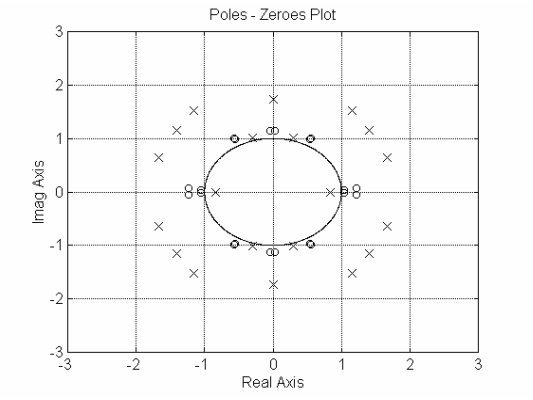

(b)

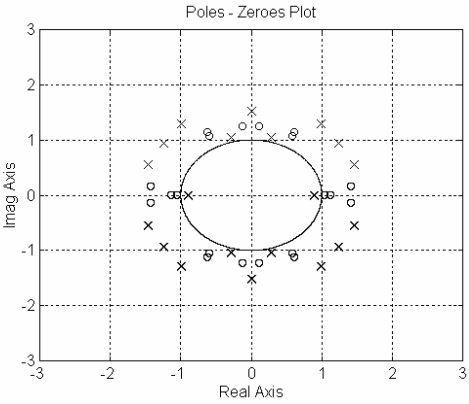

(c)

Figure 19 Pole-zero pattern for (a) $k_1=k_2=k_3=0.1$ (b) $k_1=k_2=k_3=0.2$ and (c) $k_1=k_2=k_3=0.3$

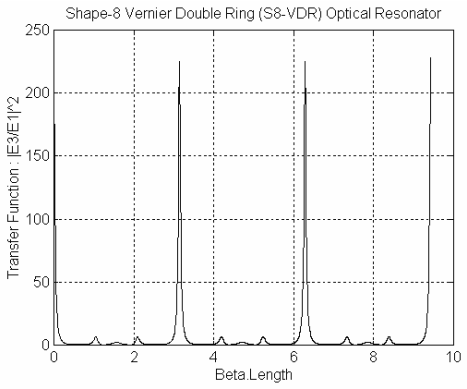

(a)

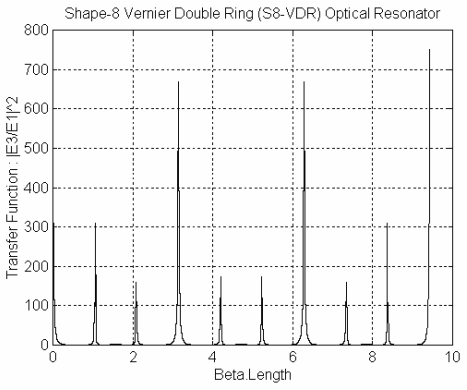

(b)

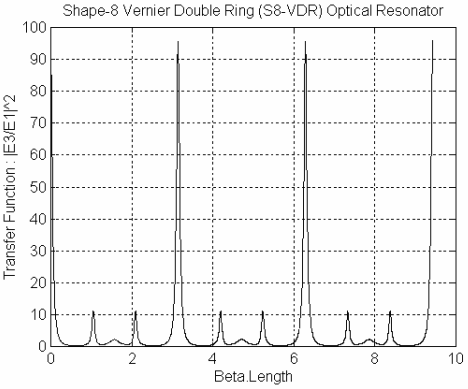

(c)

Figure 20 Optical transfer function of (a) $g_1=g_3=1$, $g_2=1.5$ (b) $g_1=g_3=1$, $g_2=2$ and (c) $g_1=g_3=1$, $g_2=2.5$.